Polymer Chemistry

ROYAL SOCIETY OF CHEMISTRY

PAPER

View Article Online
View Journal | View Issue

Check for updates

Cite this: *Polym. Chem.*, 2023, **14**, 1387

From vineyards to reshapable materials: α-CF_2 activation in 100% resveratrol-based catalyst-free vitrimers†

Florian Cuminet, *[a,b] Sébastien Lemouzy,[a] Éric Dantras,[b] Éric Leclerc,[a] Vincent Ladmiral[a] and Sylvain Caillol *[a]

Received 5th January 2023,
Accepted 24th February 2023

DOI: 10.1039/d3py00017f

rsc.li/polymers

Vitrimers are a class of polymers bridging the gap between resistant crosslinked thermosets and recyclable linear thermoplastics. The first vitrimer ever described was a polyester network requiring relatively high catalyst loadings to be reshaped. This feature raises concerns about catalysts potentially leaching out of the materials and accelerated ageing upon reprocessing cycles. Recently, strategies such as activation of the exchange reaction by inductive effects or neighboring group participation have been implemented in vitrimers allowing the production of reshapable materials which do not require a catalyst. Hence, α,α-difluoro esters proved to be very prone to transesterification owing to the strong electron-withdrawing character of the CF_2 group resulting from the very high electronegativity of fluorine. This feature implemented in polyester vitrimers enabled the synthesis of catalyst-free reshapable highly crosslinked networks. Moreover, this principle initially designed for petro-based monomers is here successfully adapted for resveratrol, a biobased polyphenol found in high concentrations in grapes and Japanese knotweed (*Reynoutria japonica*). The material presented contains 86% bio-based carbon, is catalyst-free, durable and recyclable, and features a high T_g.

Open Access Article. Published on 27 February 2023. Downloaded on 5/12/2026 6:32:05 AM.
This article is licensed under a Creative Commons Attribution-NonCommercial 3.0 Unported Licence.

Introduction

Vitrimers are a class of polymer materials which exhibit excellent mechanical properties and the ability to be reprocessed mechanically.[1,2] Ideally, they combine the best properties of thermoplastics, which are often easily recyclable, and thermosets, which are endowed with very good mechanical properties and resistance at high temperatures. These exceptional properties come from their structure. While thermoplastics are essentially a network of entangled linear chains whose cohesion is due to weak bonds, thermosets are a tridimensional network made of strong covalent bonds.[3] Vitrimers are also 3D covalent networks, but some of their bonds can undergo exchanges with each other (metathesis) or with other reactive groups located on the polymer segments, *via* a degenerate chemical reaction.[4–7] These exchanges are usually activated by heat and are accountable for the vitrimer flow and recyclability at high temperatures. Vitrimers were invented a decade ago, and first illustrated with polyesters that were able to flow, thanks to a transesterification reaction.[8] They are of particular interest in the field of composites, in which the polymer matrix needs high mechanical performances and thermal resistance[9,10] but is very challenging to reprocess.[11,12] Vitrimers, which can be reshaped upon heating and be depolymerized by solvolysis (for example), could be a solution to address the issue of composite recycling.[13–15] However, for such applications, it is desirable to obtain rigid materials with high T_g.[16–19] Thermosets with high T_g are very common, in particular when they are synthesized from the ubiquitous bisphenol A diglycidyl ether (BADGE). High T_g vitrimers are less common, even when BADGE is used.[8] Only fourteen examples of vitrimers with T_g values above 100 °C have been reported. For instance, epoxy–anhydride vitrimers catalyzed by zinc(II) with T_g values up to 140 °C have been described, but they required hard reprocessing conditions, at 250 °C under 500 bars.[20] An epoxy–acid system catalyzed by Sn(II) with 2 equivalents of epoxy with respect to the acid allowed reaching a T_g value of 231 °C thanks to the homopolymerization of the epoxy.[21] However, the resulting ether bonds cannot be reversibly cleaved under the reshaping conditions, which therefore limits the material reprocessability. Furthermore, in the case of transesterification vitrimers, an external catalyst is usually

[a]*ICGM, Univ. Montpellier, CNRS, ENSCM, Montpellier, France. E-mail: sylvain.caillol@enscm.fr, florian.cuminet@gmail.com*
[b]*CIRIMAT, Université Toulouse 3 Paul Sabatier, Physique des Polymères, 118 Route de Narbonne, 31062 Toulouse, France*

†Electronic supplementary information (ESI) available: ^1H, ^{13}C, and ^{19}F NMR spectra, TGA, DSC, DMA thermograms, EEW calculation details, and fitting parameters for stress relaxation experiments. See DOI: https://doi.org/10.1039/d3py00017f

Open Access Article. Published on 27 February 2023. Downloaded on 5/12/2026 6:32:05 AM.
This article is licensed under a Creative Commons Attribution-NonCommercial 3.0 Unported Licence.

required to accelerate the transesterification reaction, so that the material may flow at a measurable timescale and be reprocessed.[22] The use of catalysts such as zinc(II) and triazabicyclodecene (TBD) raises concerns about potential leaching of the catalysts out of the material and premature ageing of the vitrimers after several recycling/reshaping cycles.[23–25] For these reasons, the use of catalyst-free vitrimers is preferable. The first strategy is to use other exchange reactions, for instance, vinylogous urethanes,[26] polythiourethanes,[27] disulfides,[28,29] imine bonds,[30–33] silyl ethers,[34] and Si–O–Ph bonds.[35] Several other strategies were described to make catalyst-free vitrimers, in particular, in the case of transesterification vitrimers. Hyperbranched vitrimers featuring a loose network allowed catalyst-free reprocessing, but their mechanical properties were fairly limited.[36] A high concentration of free hydroxyl groups in the network also accelerates the transesterification, but it implies limitations in terms of accessible monomers and network structures and properties, and may increase the water intake of such materials.[37,38] The kinetics of the exchange reaction can also be increased by an activating group, linked to the network, in proximity to the exchangeable bonds.[39,40] In particular, fluorinated esters were recently proven to undergo fast transesterification without recourse to external catalyst, both in solution[41] and in vitrimers.[42,43] Furthermore, in the context of increasing tension on crude oil supply and price volatility, the pursuit of biobased materials is of booming interest to increase polymer sustainability.[44–46] The first vitrimer was partly biobased as the polyfunctional carboxylic acid used was made from dimers and trimers of fatty acids.[8] Many naturally occurring building blocks can be used in the synthesis of vitrimers, such as lignins, phenols, furans, oils, polysaccharides, carboxylic acids or natural rubber.[47] In particular, several examples of biobased vitrimers based on natural phenols such as vanillin,[48–50] eugenol[51,52] or cardanol[53] have been reported. However, only a few of them exhibit T_g over 100 °C and high thermal stability, two precious properties for biobased vitrimers.[54] Some examples of catalyzed biobased vitrimers with high T_g were described[55,56] but only two examples of high-T_g catalyst-free biobased vitrimers have been reported. The first example is based on acetal exchange, with a T_g up to 121 °C.[57] The other example is based on transesterification activated by tertiary amines in polybenzoxazines, with T_g ranging from 143 to 193 °C.[58] Many of the high-T_g vitrimers reported so far are based on monomers featuring aromatic structures. Biobased phenols and furans,[47] owing to their aromatic cycles and often compact structures, can provide high crosslinking density, rigidity, high T_g and thermal resistance to vitrimers.

In the work presented here, a catalyst-free, high T_g biobased transesterification vitrimer was synthesized from resveratrol, a biobased triphenol mainly found in grapes, peanuts and a plant called Japanese knotweed (*Reynoutria japonica*).[59,60] Resveratrol can be obtained from the rhizomes of this invasive plant for its valorization after uprooting.[61,62] The goal was to achieve high mechanical properties and reach high T_g thanks to the high aromatic carbon content of this bioresource. Resveratrol was functionalized to prepare two building blocks: a trifunctional epoxy and a trifunctional α,α-difluorocarboxylic acid. The rationale was that the ring-opening polyaddition of these building blocks would lead to a dense network, endowed with high T_g and transesterification capability *via* fluorinated group activation.

Results and discussion

α,α-Difluoro carboxylic acid monomer synthesis

α,α-Difluoro carboxylic acids were proven to activate the transesterification reaction in polyester networks, without the need for any catalyst, thus enabling the synthesis of catalyst-free transesterification vitrimers.[41,43] A biobased tris α,α-difluoro carboxylic acid was synthesized from resveratrol (a biobased compound extracted from grapes). Starting from the triphenol, a 2-step synthesis led to the desired monomer. Resveratrol could be easily functionalized *via* Williamson-type etherification in the presence of ethyl bromodifluoroacetate at 70 °C for 40 hours.[63,64] Dimethylformamide (DMF) was used for the feasibility study, but a 1 : 1 mixture of green solvents γ-valerolactone and dihydrolevoglucosenone (Cyrene™) could also be used as a greener alternative. After filtration on silica gel, the expected α,α-difluoro triester (**RvOEt**) was obtained in 87% yield. The isolated tris(ethyl ester) product underwent facile saponification under mild conditions to yield, after appropriate workup, the desired α,α-difluoro triacid (**RvOH-TAF**) as a brown waxy solid with an overall yield of 85% and a biobased carbon content of 70% (Scheme 1).

Trifunctional epoxy synthesis

In parallel with the modification of resveratrol into an activated trifunctional acid, this triphenol was also functionalized with epichlorohydrin to yield a trifunctional epoxy (Scheme 2).

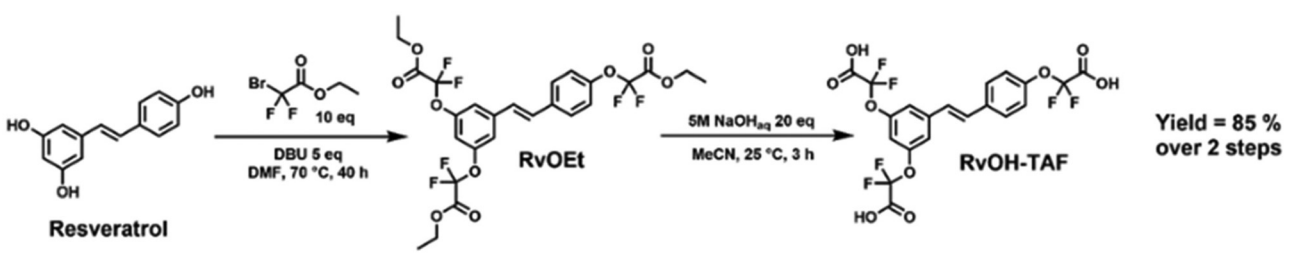

Scheme 1 2-Step synthesis of **RvOH-TAF** from resveratrol.

 This journal is © The Royal Society of Chemistry 2023

Open Access Article. Published on 27 February 2023. Downloaded on 5/12/2026 6:32:05 AM.
This article is licensed under a Creative Commons Attribution-NonCommercial 3.0 Unported Licence.

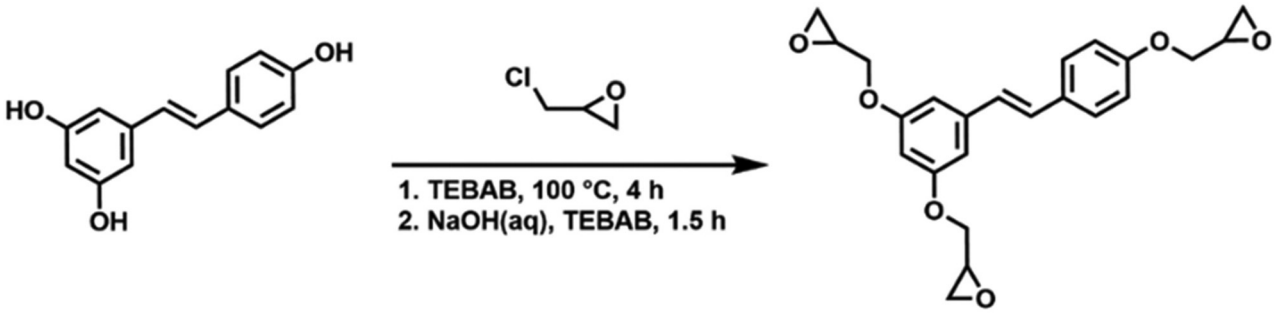

Scheme 2 Synthesis of epoxidized resveratrol **RvOGly**.

The glycidylation of phenols is very efficient and easily scalable, and was extensively described already on biobased phenols including resveratrol.[65–68] The targeted building block **RvOGly** was prepared in large quantities (>40 g) by a simple reaction of resveratrol with epichlorohydrin and tetrabutylammonium bromide (TEBAB). **RvOGly** features high functionality (EEW = 185 g per eq.) and a 52% aromatic carbon content (for **RvOGly** alone), close to the 57% value of bisphenol A diglycidyl ether (BADGE), two features which are beneficial for obtaining materials with high T_g.

Polymerization and curing

RvOGly and **RvOH-TAF** were mixed at room temperature (*ca.* 20 °C) in PTFE molds to avoid any transfer step, because of the fast gelation of the mixture even at room temperature (*ca.* 20 °C). The reaction between both monomers was exothermic and the mixing step needed to be performed on a small scale, typically 1–2 g, to better control the heat transfer and to avoid gelation before complete mixing. This fast gelation is caused by the strong activation of the carboxylic acids toward the epoxy opening by the fluorine atoms. A reaction on larger scales may benefit from the addition of a solvent to control the heat release. This pathway was not explored in this study though, to avoid the plasticizing effect of the potential residual solvent and its effect on mechanical properties. The mixture formed a material within a few minutes, and was maintained at room temperature for 3 h.

The curing was checked by DSC (Fig. S9†). On the first heating ramp, an exothermic enthalpy is observed starting from 150 °C. On the second ramp, this phenomenon does not appear and a T_g is observed in the 100–130 °C range. The exothermic phenomenon was attributed to a residual polymerization occurring when the material is heated higher than 150 °C. This is not surprising, since the T_g of the reactive system increases as it undergoes polymerization. When the T_g equals the temperature at which the reaction occurs, the reaction is frozen because of vitrification. It is necessary to heat above the T_g at the maximal conversion to complete the polymerization. Thus, a 1 h curing step at 150 °C was applied and the DSC analysis was repeated (Fig. S10†). After this curing step, two consecutive heating ramps overlaid almost perfectly. There was no sign of ongoing polymerization by DSC. The curing was also checked by mechanical analysis. The evolution of the modulus was monitored with time at 150 °C. The stabilization of the value happened after 7 h (Fig. S11†). Therefore, the materials were maintained at 150 °C for 10 h to ensure complete polymerization, resulting in a hard brittle dark brown material (**Vm-RvOH**, Fig. 1). The resulting material exhibits an 86% biobased carbon content.

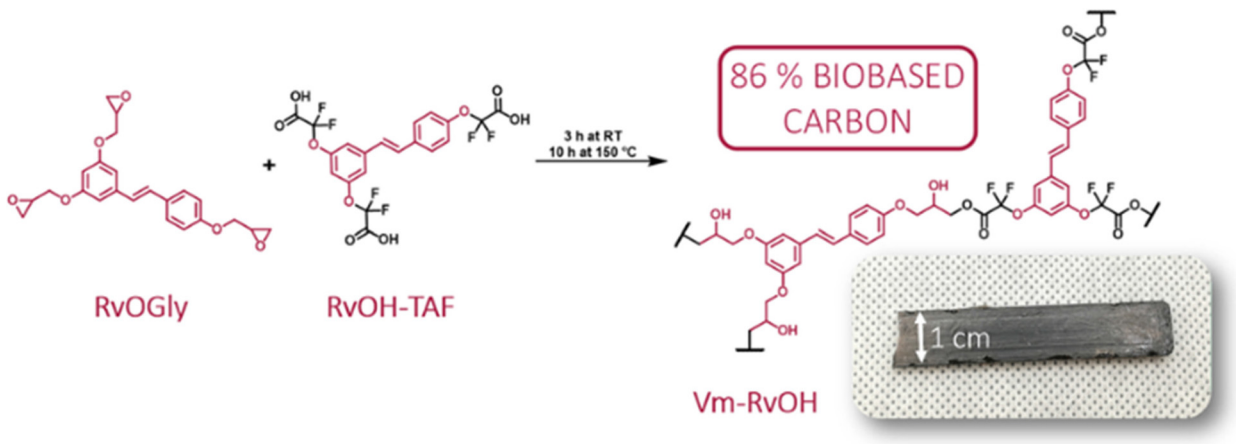

Fig. 1 Polymerization of **RvOGly** and **RvOH-TAF** resulting in the **Vm-RvOH** material, inset: an optical image of **Vm-RvOH** (1 cm × 4.5 cm × 0.3 cm).

Open Access Article. Published on 27 February 2023. Downloaded on 5/12/2026 6:32:05 AM.
This article is licensed under a Creative Commons Attribution-NonCommercial 3.0 Unported Licence.

Vitrimer characterization

After complete polymerization three consecutive DSC ramps were carried out on the resulting material. The first ramp was meant to erase the thermal history of the material, then the thermograms of the second and third ramps overlaid perfectly, and no residual exotherm was observed. The T_g is observed in the 92–125 °C range, but the transition is broad and the ΔC_p is low (0.241 J g^{-1} K^{-1}). Therefore, the T_g was determined as the minimum of the heat flow derivative, at 117 °C (Fig. S12† and Table 1). The high T_g compared to those of previously reported covalent adaptable networks[42,43] was expected because of the high aromatic carbon content of the polymer (56% aromatic carbon content for the polymer). This value of T_g is comparable to that of a catalyst-free biobased vitrimer synthesized from lignin by Moreno *et al.*[57] (T_g = 121 °C), but lower than the value of the catalyst-free biobased polybenzoxazine vitrimers recently reported by Adjaoud *et al.* (T_g from 143 to 193 °C).[17] This last case benefits from a 50% aromatic carbon content, close to the 56% value reported here, and also a 17% cycloaliphatic carbon content caused by the isosorbide core of its monomer, which brings additional rigidity. Thus, the performance of **Vm-RvOH** in terms of T_g is consistent with its structure.

DMA analysis was also performed to confirm the results observed by DSC and to characterize the mechanical properties of the material (Fig. S13†). T_α was determined as the maximum of the loss modulus E'' at 94 °C. As observed by DSC, the mechanical relaxation was broad and the temperature of the maximum of tan(δ) was 117 °C, which is consistent with the T_g measured by DSC. The moduli on the glassy plateau and on the rubbery plateau were respectively E'_G = 2.1 GPa and E'_R = 46 MPa. The modulus on the glassy plateau is comparable to values reported for a material made from epoxidized resveratrol and 4,4′-diaminodicyclohexylmethane (PACM),[68] and with the value of a lignin-based catalyst-free vitrimer.[57] As for the modulus on the rubbery plateau, the value for **Vm-RvOH** is 14 times lower than that of an epoxidized resveratrol-PACM thermoset,[68] but still in the 11–73 MPa range reported for other high-T_g vitrimers,[18,21] included for aerospace applications.[29] Additionally, this value is 2.5 times higher than the value reported on a similar α,α-difluoro vitrimer previously reported.[43] At temperatures over 200 °C, the modulus decreases from the rubbery plateau. This could be the manifestation of the beginning of the flow.

The thermal stability of **Vm-RvOH** was assessed by TGA under nitrogen. The 2% and 5% degradation temperatures $T_{d\,2\%}$ and $T_{d\,5\%}$ were 237 °C and 275 °C respectively (Fig. S14† and Table 1). The residue at 900 °C under nitrogen was 28.9% of the initial weight. The $T_{d\,5\%}$ value is low compared to the values above 300 °C reported for other high-T_g vitrimers,[18,32,33,35,56,69] but still higher than the value at 224 °C for a lignin-based catalyst-free vitrimer.[57] The residue (char yield) was comparable with an epoxy vitrimer in the same range of T_g.[31] The relatively high char yield depends essentially on the monomer structures, thanks to the high aromatic carbon content (56%).

Solubility tests were performed in THF (which easily solubilizes both resveratrol-based precursors). After stirring for 24 hours, a swelling of 278% and an insoluble fraction of 73 ± 2% were measured. This result seemed low for a 3 + 3 cross-linked material, and might be attributed to hydrolysis due to water in THF. Therefore, it was repeated in anhydrous THF. A swelling of 68% and a gel content of 100 ± 1% were found (Table 1). These results prove the formation of a 3D cross-linked material.

Reprocessing trials were performed on **Vm-RvOH** by compression molding. In a previous study on a similar system, the reprocessing temperature was set at 100 °C, 50 °C above the T_g, under 16 bars.[43] At 170 °C, the material could be reprocessed in 2 h under 80 bars (Fig. 2). The reprocessing temperature is 50 °C above the T_g, like the previous system. The pressure applied is lower than that for many high-T_g vitrimers, which often require a pressure of at least 100 bars.[28,32,35,56,70]

The thermal stability of the material at this reprocessing temperature was assessed. An isothermal experiment at 170 °C was performed under an air atmosphere, to simulate the reprocessing conditions (Fig. S15†). After 2 h, the relative mass loss was 2.48%. Between 2 h and 4 h the additional mass loss was 0.29% and between 4 h and 6 h, it was 0.47%, attaining an overall mass loss of around 3% after 6 h. This value is small, but cannot be ignored. Reprocessing trials were made at 170 °C under 80 bars. Therefore, the DMA analysis of the material needs to be assessed, and compared before and after reprocessing at 170 °C to monitor possible degradation. Two consecutive reprocessing cycles at 170 °C were performed, and the mechanical properties after each cycle were studied by DMA (Fig. 3).

The value of the modulus on the glassy plateau remains quasi-constant. The value of T_α decreased from 94 to 75 °C after the first reprocessing cycle, and remained at 76 °C after the second cycle (Table 2). Similarly, the values of the modulus on the rubbery plateau E'_R decreased from 46 to 23 MPa with the first reprocessing, and then remained the same after the second cycle. These results suggest a decrease of the cross-

Table 1 Physicochemical main properties of **Vm-RvOH**

T_g (°C)	T_α[a] (°C)	Max. tan(δ) (°C)	E'_G[b] (GPa)	E'_R[c] (MPa)	Gel content[d] (%)	Swelling index[d] (%)	$T_{d\,2\%}$[e] (°C)	$T_{d\,5\%}$[e] (°C)	Residue (char)[f] (%)	Weight loss[g] (%)
117	94	117	2.1	46	100 ± 1	68	237	275	28.9	2.9

[a] Determined as the maximum of E''. [b] At T_α − 50 °C. [c] At T_α + 50 °C. [d] In anhydrous THF. [e] N_2 atmosphere. [f] At 900 °C, N_2 atmosphere. [g] After 6 h at 170 °C, air atmosphere.

This journal is © The Royal Society of Chemistry 2023

Open Access Article. Published on 27 February 2023. Downloaded on 5/12/2026 6:32:05 AM.
This article is licensed under a Creative Commons Attribution-NonCommercial 3.0 Unported Licence.

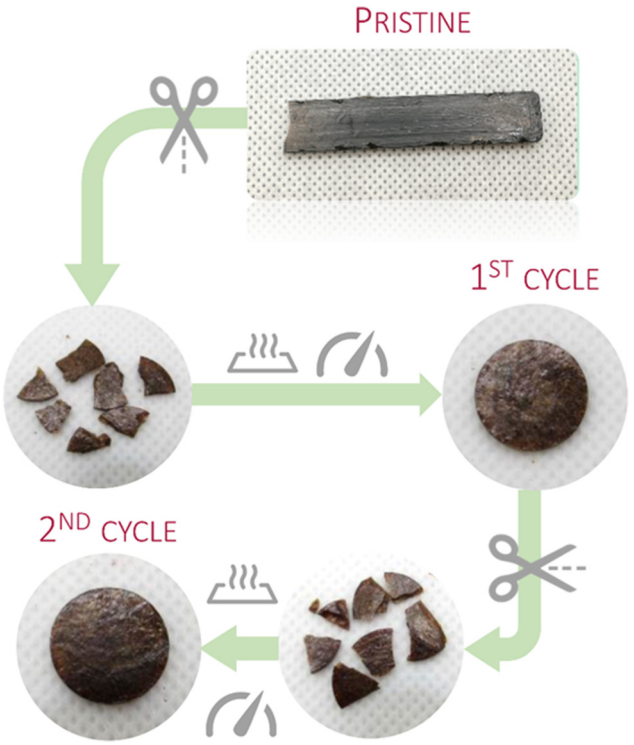

Fig. 2 **Vm-RvOH** reprocessing for 2 h at 170 °C under 80 bars (scale of pristine material: 1 cm × 4.5 cm × 0.3 cm, diameter of reprocessed materials: 1 cm).

linking density upon the first cycle, which might be due to a slight hydrolysis at the reprocessing temperature. Then the crosslinking density remains constant for the subsequent cycle, and thus the hydrolysis remains very limited. This is likely due to the aromatic carbon content (56% aromatic carbon), which brings a hydrophobic behavior to the material and balances the hydrophilic behavior brought by the esters and hydroxyl groups. Moreover, the high T_g probably plays an important role, as the water uptake is very limited when the material is in the glassy state, but much easier in the rubbery state. Indeed, in the rubbery state, the mobility of the polymer makes the penetration of water into the network easier. Finally, the results obtained by DMA were confirmed by DSC, with a T_g of 117 °C for the pristine material, 97 °C after the first reprocessing and 91 °C after the second cycle.

The flow from the rubbery plateau was studied by isothermal stress-relaxation experiments to evaluate the kinetics of this phenomenon (Fig. S16†). The modulus of the material was monitored under 0.3% strain between 170 and 210 °C. For all temperatures, a plateau at around 5% was reached at the end of the relaxation experiment. This is likely due to a proportion of permanent linkages in the network. The presence of such permanent linkages can be explained by a minor homopolymerization of the epoxy.[21] Indeed, the strong acidity of α,α-difluoro acids may favor this reaction.[21]

The stress-relaxation experiments were normalized, and a Kohlrausch–Williams–Watts "stretched exponential" equation with an added constant y_0 was used to fit the experimental

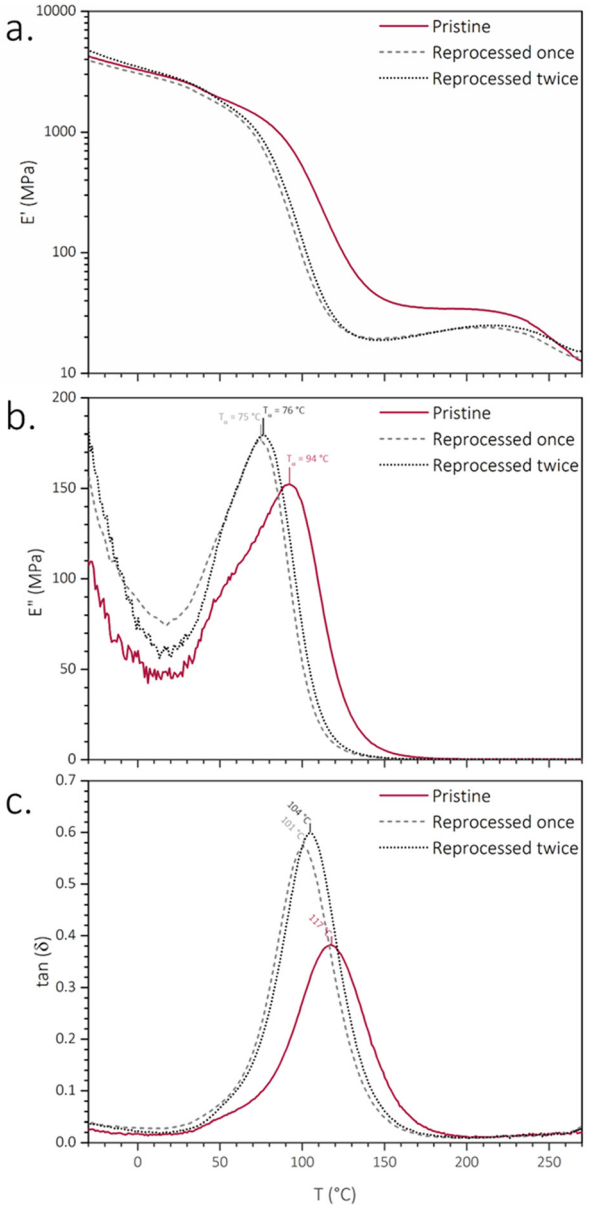

Fig. 3 DMA thermograms (a) E', (b) E'' and (c) tan(δ) of **Vm-RvOH** pristine, after one reprocessing cycle and after two reprocessing cycles.

Table 2 Evolution of the thermomechanical properties of **Vm-RvOH** with reprocessing cycles

Reprocessing cycle	T_g (°C)	T_α[a] (°C)	Max. tan(δ) (°C)	E'_G[b] (GPa)	E'_R[c] (MPa)
Pristine	117	94	117	2.1	46
Reprocessed once	97	75	101	2.4	23
Reprocessed twice	91	76	104	2.7	23

[a] Determined as the maximum of E''. [b] At $T_\alpha - 50$ °C. [c] At $T_\alpha + 50$ °C.

data (Fig. 4 and Table S1†). The constant y_0 translates the final plateau of the relaxation, and the stretch parameter β translates a distribution of behaviors centered on the value of the

Open Access Article. Published on 27 February 2023. Downloaded on 5/12/2026 6:32:05 AM.
This article is licensed under a Creative Commons Attribution-NonCommercial 3.0 Unported Licence.

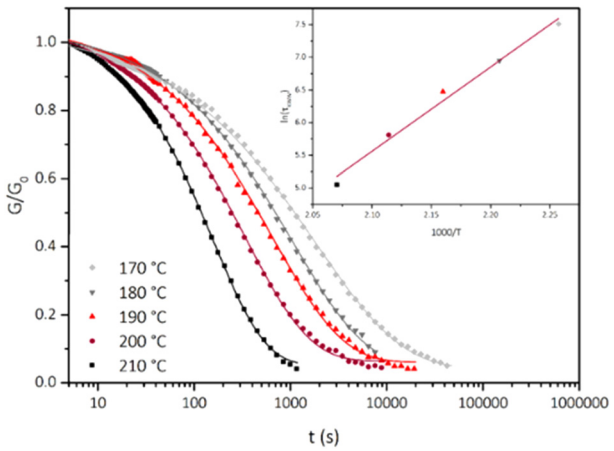

Fig. 4 Normalized stress–relaxation curves from 170 to 210 °C with 10 °C steps fitted with the Kohlrausch–Williams–Watts equation (KWW) and τ_{KWW} relaxation times reported in the Arrhenius diagram (inset, R^2 = 0.983).

relaxation time τ_{KWW}. The closer to 1 the β is, the narrower the distribution is. This parameter is linked to the heterogeneity in the vicinity of the exchangeable bond. Here, the values of β ranged between 0.486 at 170 °C and 0.797 at 210 °C, and increased with the temperature. The broad distribution might be due to the influence of weak bonds hindering the relaxation. The number of weak bonds probably decreased when the temperature increased, which would result in an increasingly homogeneous behavior of the exchangeable bonds, and the increasing value of β. The constant added y_0 allowed better accuracy on the fitting, with $0.99264 \leq R^2 \leq 0.99639$ without the constant and R^2 = 0.99937 to 0.99979 with the constant. The mean value of this constant y_0 (Table S1†) is 0.054 (values are between 0.043 and 0.064). Thus, mere 5% of the applied stress is not relaxed because of the permanent linkages, which does not impede the reprocessing of the material.

The relaxation times τ_{KWW} obtained for each temperature were plotted in an Arrhenius diagram (Fig. 4 inset). A linear fit was obtained (R^2 = 0.983) and the flow activation was calculated from the slope E_a = 107 kJ mol^{-1}, in accordance with the 29–163 kJ mol^{-1} range reported for transesterification vitrimers.[40] This E_a is higher than that reported in previous studies of transesterification vitrimers activated by fluorinated groups (67–77 kJ mol^{-1}).[42,43] It is likely caused by the higher crosslinking density and lower mobility at the local scale of **Vm-RvOH**.

Conclusions

A catalyst-free polyester vitrimer was synthesized from resveratrol, a biobased triphenol found mainly in grapes. This material exhibits a high biobased carbon content of 86%. A trifunctional epoxy and a trifunctional α,α-difluoro carboxylic acid were synthesized by functionalization of resveratrol with epichlorohydrin and ethyl bromodifluoroacetate, respectively. When these two resveratrol derivatives were mixed together, the ring opening polymerization of the epoxy by the carboxylic acid occurred at room temperature owing to the increased acidity of the carboxylic acid O–H bond due to the neighboring electronegative fluorine atoms. After a curing step at 150 °C, a rigid slightly brittle material was obtained. This material exhibited a high T_g (117 °C), comparable to other high-T_g vitrimers,[28,31,71,72] which makes it relevant for structural applications. The synthesis described could be adapted to other biobased compounds with similar structures and higher functionality, such as quercetin, to achieve even higher T_g values. Moreover, the α,α-difluoro esters can exchange with free hydroxyl groups without any added catalyst. This feature allows the efficient reprocessing of the material at 170 °C for 2 h by compression molding. Two recycling cycles were achieved and the mechanical performance remained worthwhile for structural applications. This material is one of the first high-T_g catalyst-free biobased vitrimers.[17,57]

Experimental section

Materials

trans-Resveratrol (Fluorochem, 98%), 1,8-diazabicyclo(5.4.0)undec-7-ene (DBU, Fluorochem, 98%), ethyl bromodifluoroacetate (Fluorochem, 98%), epichlorohydrin (Sigma-Aldrich, ≥99%), tetrabutylammonium bromide (TCI, >98%), and benzophenone (Avocado Research Chemicals Ltd, 99%) were used as received. Dimethylformamide (DMF, ≥99.5%), tetrahydrofuran (THF, ≥99%) and $NaHCO_3$ were supplied by VWR Chemicals; diethyl ether (≥99.5%) and pentane (≥95%) were supplied by Carlo Erba; ethyl acetate (≥99%) was supplied by Fisher Chemicals; acetonitrile (≥99.9%) was supplied by Acros Organics; sodium hydroxide (≥98%) and chlorohydric acid ≥ 37% were supplied by Honeywell Fluka; anhydrous THF was supplied by Carlo Erba (anhydrous for analysis stabilized with BHT, on 4A molecular sieves). Deuterated solvents were supplied by Eurisotop (99.8%). γ-Valerolactone (GVL, BioRenewable, ≥99%) and dihydrolevoglucosenone (Cyrene™, BioRenewable, ≥98.5%) were obtained from Sigma-Aldrich.

Synthetic procedures

"RvOEt" compound[63,64]*. *trans*-Resveratrol (3,5,4′-trihydroxy-*trans*-stilbene, 2.3 g, 10 mmol, 1 eq.) was dissolved in dry DMF (60 mL, 0.16 M). 1,8-Diazabicyclo[5.4.0]undec-7-ene (DBU, 7.5 mL, 50 mmol, 5 eq.) was added in one portion and the reaction was heated to 70 °C. Ethyl bromodifluoroacetate (6.4 mL, 50 mmol, 5 eq.) was then added *via* a syringe pump at a rate of 5.0 mL h^{-1} and the reaction mixture was stirred at 70 °C for 40 h. The crude mixture was cooled to room temperature, diluted with H_2O (300 mL), and extracted 5 times with Et_2O (5 × 50 mL). The combined organic layers were washed twice with water and once with brine, dried with Na_2SO_4, filtered, and concentrated under reduced pressure to obtain dark red oil. The crude mixture was purified by filtration on silica

This journal is © The Royal Society of Chemistry 2023

Open Access Article. Published on 27 February 2023. Downloaded on 5/12/2026 6:32:05 AM. This article is licensed under a Creative Commons Attribution-NonCommercial 3.0 Unported Licence.

gel using pentane/ethyl acetate (1 : 1) to afford the pure triester (6 g, 87%, clear brown viscous liquid).

Triester **RvOEt** characterization (NMR spectra in Fig. S1–S3†): ^{1}H NMR 400 MHz $CDCl_3$: δ 7.50 (m, 2H, aromatic protons), 7.25–7.21 (m, 4H, aromatic protons and C=C), 7.11–6.95 (m, 3H, aromatic protons), 4.40 (2q, ^3J = 8 Hz, 6H, $OC\underline{H}_2CH_3$), 1.37 (2t, ^3J = 8 Hz, 9H, $OCH_2C\underline{H}_3$). ^{19}F NMR 377 MHz, $CDCl_3$: δ −76.30, −76.53. ^{13}C NMR 101 MHz, $CDCl_3$: δ 159.9 (m, $\underline{C}O_2Et$), 150.3 (m), 150.2 (m), 140.1, 134.7, 130.3, 128.1, 127.1, 122.0, 117.4, 114.1 (t, $^1J_{C-F}$ = 1021 Hz, OCF_2), 114.0 (t, $^1J_{C-F}$ = 1025 Hz, OCF_2), 64.0 (O–$\underline{C}H_2CH_3$), 63.9 (O–$\underline{C}H_2CH_3$), 14.0 (O–$CH_2\underline{C}H_3$), 14.0 (O–$CH_2\underline{C}H_3$). HRMS (ESI$^+$) calc. for $[M + H]^+$ 595.1397, found 595.1394.

"RvOH-TAF" compound. In a 250 mL round bottom flask, 6 g of triester were dissolved in acetonitrile (90 mL). Then, a 5 M aqueous solution of NaOH (12.5 g in 62 mL) was added slowly at room temperature, and the mixture was stirred for 3 h. 200 mL of a saturated $NaHCO_3$ solution was added to the mixture and the aqueous layer was washed with 100 mL of diethyl ether. The organic layer was extracted with 50 mL of saturated $NaHCO_3$ solution, and the gathered aqueous layers were acidified to pH = 1 using 2 M HCl. Finally, the acidified aqueous layer was extracted with 3 × 100 mL of diethyl ether, and the solvent was removed under high vacuum to afford 5 g of the desired triacid as a brown waxy solid (yield 98%, yield over the two steps η = 85%, purity > 98% estimated from the ^{1}H NMR spectrum).

Trifunctional acid TPE-TAF characterization (NMR spectra in Fig. S4–S6†): ^{1}H NMR 400 MHz d_6-DMSO: δ 7.72 (d, 2H), 7.59–7.13 (m, 5H, aromatic protons and C=C), 7.00 (s, 1H). ^{19}F NMR 377 MHz, d_6-DMSO: δ −76.16, −76.50. ^{13}C NMR 101 MHz, d_6-DMSO: δ 161.0 (COOH, t, $^2J_{C-F}$ = 39.0 Hz), 160.7 (COOH, t, $^2J_{C-F}$ = 39.0 Hz), 150.4 (*ipso*-ArC–O), 149.4, 140.8, 135.0, 130.6, 128.7, 127.1, 121.8, 117.3, 114.64 (OCF_2, t, $^1J_{C-F}$ = 272 Hz), 114.56 (OCF_2, t, $^1J_{C-F}$ = 274 Hz), 113.4. HRMS (ESI$^+$) calc. for $[M + H]^+$ 511.0458, found 511.0468. HRMS (ESI$^-$) calc. for $[M - H]^-$ 509.0313, found 509.0319.

"RvOGly" compound (glycidylation of resveratrol). In a 500 mL round bottom flask, 20.56 g (90 mmol, 1 eq.) of resveratrol was dissolved in 82 mL (96 g, 1.04 mol, 12 eq.) of epichlorohydrin at room temperature under magnetic stirring. The flask was then equipped with a condenser and heated to 100 °C. 1.56 g (4.8 mmol, 0.05 eq.) of tetrabutylammonium bromide "TEBAB" was added and the reaction was left to proceed under stirring at 100 °C for 4 h. Then, the reaction medium was cooled to room temperature, and 20 wt% aqueous solution of NaOH and TEBAB was added (21 g NaOH + 1.56 g TEBAB in 106 mL deionized water). The mixture was left under vigorous stirring for 1.5 h. The mixture was then diluted with 600 mL of water and extracted with 3 × 300 mL ethyl acetate. The organic layers were gathered, washed with 2 × 200 mL of brine, and dried on magnesium sulfate. The solvent was evaporated under reduced pressure to afford 42.3 g of clear yellow viscous oil.

Epoxidized resveratrol **RvOGly** characterization (NMR spectra in Fig. S7 and S8†): ^{1}H NMR 400 MHz d_6-acetone: δ 7.52 (d, 2H), 7.29–6.99 (dd, 2H, C=C), 6.97 (m, 2H), 6.81 (d, 2H), 6.51 (t, 1H), 4.34 and 3.86 (3 + 3H), 3.33 (3H), 2.86 and 2.73 (3 + 3H). ^{13}C NMR 101 MHz, d_6-acetone: δ 160.9, 159.3, 140.7, 131.0, 129.5, 128.6, 127.1, 115.5, 106.0, 101.3, 70.1, 50.6, 44.4.

Determination of the epoxy equivalent weight (EEW). The EEW of **RvOGly** was evaluated by NMR titration using benzophenone as the standard in deuterated chloroform (experimental details are given in the ESI Section A†).

"TPE-TAF/BDGE" vitrimer. Typically, 1 g (2.0 mmol, 5.9 meq. COOH, HEW = 170 g per eq.) of **RvOH-TAF** was quickly mixed manually and directly in a PTFE mold with 1.07 g (5.9 meq. epoxy, EEW = 185 g per eq.) of **RvOGly** at room temperature (*ca.* 20 °C) until a light brown viscous homogeneous mixture was obtained. The mixture was maintained for at least 3 h at room temperature for gelation. The resulting material (TPE-TAF/BDGE) was then removed from the molds and cured for 10 h at 150 °C.

Instrumentation

NMR. ^{1}H, ^{13}C and ^{19}F NMR spectra were acquired on a Bruker Avance 400 MHz spectrometer at 23 °C. External reference was tetramethylsilane (TMS) with chemical shifts given in ppm. Samples were diluted in 0.5 mL of $CDCl_3$, DMSO-d_6 or acetone-d_6 depending on their solubility.

Mechanical characterization. Temperature ramps in the elongation mode were carried out on a Netzsch DMA 242 E Artemis cooled with liquid nitrogen. Uniaxial stretching of samples (1 × 3.5 × 12 mm^3) was applied while heating at a rate of 3 °C min^{-1} from −50 °C to 270 °C, keeping the frequency at 1 Hz. Curing monitoring experiments were performed on a ThermoScientific Haake Mars 60 rheometer equipped with a Peltier heating cell and an 8 mm plane–plane geometry. A 0.1% deformation was applied to 8 mm diameter and 2 mm thickness circular samples at ω = 1 rad s^{-1} under a normal force of 100 grams for every 2 minutes, and G' evolution over time was monitored. Stress relaxation experiments were performed with 0.3% torsional strain applied on 8 mm diameter and 2 mm thickness circular samples, and the rubbery modulus evolution with time was monitored.

TGA. Thermogravimetric thermograms were recorded on a TA TGA G50 instrument using a 40 mL min^{-1} flux of nitrogen or synthetic air as purge gas. Approximately 10 mg of samples were used for each analysis. Ramps were applied at a rate of 20 °C min^{-1}.

DSC. Analyses were carried out using a NETZSCH DSC200F3 calorimeter. The calibration was performed using adamantane, biphenyl, indium, tin, bismuth and zinc standards. Nitrogen was used as purge gas. Approximately 10 mg of samples were placed in perforated aluminum pans and the thermal properties were recorded at 20 °C min^{-1}. The reported values are the values measured during the second heating ramp.

Reprocessing. The material was ground with a manual stainless steel coffee grinder (for DSC and DMA) or cut into 6 to 9 mm^3 pieces (for pictures) and then pressed in stainless steel

Open Access Article. Published on 27 February 2023. Downloaded on 5/12/2026 6:32:05 AM. This article is licensed under a Creative Commons Attribution-NonCommercial 3.0 Unported Licence.

molds for 2 h at 170 °C under 80 bars pressure using a manual heating press.

Author contributions

Conceptualization: FC, SC, ED, SL, EL and VL. Funding acquisition: SC, ED, EL and VL. Investigation: FC and SL. Methodology: all authors. Project administration: SC, ED, EL and VL. Supervision: FC, SC, ED, EL and VL. Validation: all authors. Visualization: FC. Writing – original draft: FC. Writing – review & editing: all authors.

Conflicts of interest

There are no conflicts to declare.

Acknowledgements

This work was funded by the Institut Carnot Chimie Balard CIRIMAT (16CARN000801).

Notes and references

1 W. Denissen, J. M. Winne and F. E. Du Prez, *Chem. Sci.*, 2016, **7**, 30–38.
2 N. J. Van Zee and R. Nicolaÿ, *Prog. Polym. Sci.*, 2020, **104**, 101233.
3 J.-P. Pascault, H. Sautereau, J. Verdu and R. J. J. J. Williams, *Thermosetting Polymers*, Marcel Dekker, Inc., New York, 2002.
4 M. Capelot, D. Montarnal, F. Tournilhac and L. Leibler, *J. Am. Chem. Soc.*, 2012, **134**, 7664–7667.
5 L. Leibler, M. Rubinstein and R. H. Colby, *Macromolecules*, 2002, **24**, 4701–4707.
6 C. J. Kloxin, T. F. Scott, B. J. Adzima and C. N. Bowman, *Macromolecules*, 2010, **43**, 2643–2653.
7 C. J. Kloxin and C. N. Bowman, *Chem. Soc. Rev.*, 2013, **42**, 7161–7173.
8 D. Montarnal, M. Capelot, F. Tournilhac and L. Leibler, *Science*, 2011, **334**, 965–968.
9 R. Hsissou, R. Seghiri, Z. Benzekri, M. Hilali, M. Rafik and A. Elharfi, *Compos. Struct.*, 2021, **262**, 113640.
10 J. Zheng, Z. M. Png, S. H. Ng, G. X. Tham, E. Ye, S. S. Goh, X. J. Loh and Z. Li, *Mater. Today*, 2021, **51**, 586–625.
11 Y. Yang, R. Boom, B. Irion, D. J. van Heerden, P. Kuiper and H. de Wit, *Chem. Eng. Process.*, 2012, **51**, 53–68.
12 A. E. Krauklis, C. W. Karl, A. I. Gagani and J. K. Jørgensen, *J. Compos. Sci.*, 2021, **5**, 28.
13 D. A. Kissounko, P. Taynton and C. Kaffer, *Reinf. Plast.*, 2018, **62**, 162–166.
14 Y. Yang, Y. Xu, Y. Ji and Y. Wei, *Prog. Mater. Sci.*, 2021, **120**, 100710.
15 W. Alabiso and S. Schlögl, *Polymers*, 2020, **12**, 1660.
16 Y. Yang and M. W. Urban, *Chem. Soc. Rev.*, 2013, **42**, 7446–7467.
17 A. Adjaoud, L. Puchot and P. Verge, *ACS Sustainable Chem. Eng.*, 2022, **10**, 594–602.
18 T. Liu, C. Hao, S. Zhang, X. Yang, L. Wang, J. Han, Y. Li, J. Xin and J. Zhang, *Macromolecules*, 2018, **51**, 5577–5585.
19 B. P. Chang, A. K. Mohanty and M. Misra, *RSC Adv.*, 2020, **10**, 17955–17999.
20 M. Giebler, C. Sperling, S. Kaiser, I. Duretek and S. Schlögl, *Polymers*, 2020, **12**, 1148.
21 K. Tangthana-Umrung, Q. A. Poutrel and M. Gresil, *Macromolecules*, 2021, **54**, 8393–8406.
22 M. Capelot, M. M. Unterlass, F. Tournilhac and L. Leibler, *ACS Macro Lett.*, 2012, **1**, 789–792.
23 J. Wang, S. Chen, T. Lin, J. Ke, T. Chen, X. Wu and C. Lin, *RSC Adv.*, 2020, **10**, 39271–39276.
24 J. J. Lessard, L. F. Garcia, C. P. Easterling, M. B. Sims, K. C. Bentz, S. Arencibia, D. A. Savin and B. S. Sumerlin, *Macromolecules*, 2019, **52**, 2105–2111.
25 C. He, S. Shi, D. Wang, B. A. Helms and T. P. Russell, *J. Am. Chem. Soc.*, 2019, **141**, 13753–13757.
26 G. M. Scheutz, J. J. Lessard, M. B. Sims and B. S. Sumerlin, *J. Am. Chem. Soc.*, 2019, **141**, 16181–16196.
27 F. Gamardella, S. De la Flor, X. Ramis and A. Serra, *React. Funct. Polym.*, 2020, **151**, 104574.
28 L. Zhou, G. Zhang, Y. Feng, H. Zhang, J. Li and X. Shi, *J. Mater. Sci.*, 2018, **53**, 7030–7047.
29 A. Ruiz de Luzuriaga, N. Markaide, A. M. Salaberria, I. Azcune, A. Rekondo and H. J. Grande, *Polymers*, 2022, **14**, 3180.
30 H. Zheng, Q. Liu, X. Lei, Y. Chen, B. Zhang and Q. Zhang, *J. Polym. Sci., Part A: Polym. Chem.*, 2018, **56**, 2531–2538.
31 H. Liu, H. Zhang, H. Wang, X. Huang, G. Huang and J. Wu, *Chem. Eng. J.*, 2019, **368**, 61–70.
32 X. Zhang, Y. Eichen, Z. Miao, S. Zhang, Q. Cai, W. Liu, J. Zhao and Z. Wu, *Chem. Eng. J.*, 2022, **440**, 135806.
33 X. Lei, Y. Jin, H. Sun and W. Zhang, *J. Mater. Chem. A*, 2017, **5**, 21140–21145.
34 Y. Nishimura, J. Chung, H. Muradyan and Z. Guan, *J. Am. Chem. Soc.*, 2017, **139**, 14881–14884.
35 S. Gao, Y. Liu, S. Feng and Z. Lu, *J. Mater. Chem. A*, 2019, **7**, 17498–17504.
36 J. Han, T. Liu, C. Hao, S. Zhang, B. Guo and J. Zhang, *Macromolecules*, 2018, **51**, 6789–6799.
37 T. Liu, S. Zhang, C. Hao, C. Verdi, W. Liu, H. Liu and J. Zhang, *Macromol. Rapid Commun.*, 2019, **40**, 1800889.
38 F. I. Altuna, V. Pettarin and R. J. J. Williams, *Green Chem.*, 2013, **15**, 3360–3366.
39 F. I. Altuna, C. E. Hoppe and R. J. J. Williams, *Eur. Polym. J.*, 2019, **113**, 297–304.
40 F. Cuminet, S. Caillol, É. Dantras, É. Leclerc and V. Ladmiral, *Macromolecules*, 2021, **54**, 3927–3961.
41 S. Lemouzy, F. Cuminet, D. Berne, S. Caillol, V. Ladmiral, R. Poli and E. Leclerc, *Chem. – Eur. J.*, 2022, **28**, e202201135.

 This journal is © The Royal Society of Chemistry 2023

Open Access Article. Published on 27 February 2023. Downloaded on 5/12/2026 6:32:05 AM.
This article is licensed under a Creative Commons Attribution-NonCommercial 3.0 Unported Licence.

42 D. Berne, F. Cuminet, S. Lemouzy, C. Joly-Duhamel, R. Poli, S. Caillol, E. Leclerc and V. Ladmiral, *Macromolecules*, 2022, **55**, 1669–1679.
43 F. Cuminet, D. Berne, S. Lemouzy, E. Dantras, C. Joly-Duhamel, S. Caillol, E. Leclerc and V. Ladmiral, *Polym. Chem.*, 2022, **8**, 5255–5446.
44 R. P. Babu, K. O'Connor and R. Seeram, *Prog. Biomater.*, 2013, **2**, 8.
45 H. Nakajima, P. Dijkstra and K. Loos, *Polymers*, 2017, **9**, 523.
46 S. Caillol, *Natural Polymers and Biopolymers II*, MDPI, Basel, 2021.
47 M. A. Lucherelli, A. Duval and L. Avérous, *Prog. Polym. Sci.*, 2022, **127**, 101515.
48 S. Engelen, A. A. Wróblewska, K. De Bruycker, R. Aksakal, V. Ladmiral, S. Caillol and F. E. Du Prez, *Polym. Chem.*, 2022, **13**, 2665–2673.
49 A. Genua, S. Montes, I. Azcune, A. Rekondo, S. Malburet, B. Daydé-Cazals and A. Graillot, *Polymers*, 2020, **12**, 1–14.
50 Y. Y. Liu, J. He, Y. D. Li, X. L. Zhao and J. B. Zeng, *Compos. Commun.*, 2020, **22**, 100445.
51 C. Ocando, Y. Ecochard, M. Decostanzi, S. Caillol and L. Avérous, *Eur. Polym. J.*, 2020, **135**, 109860.
52 T. Liu, C. Hao, L. Wang, Y. Li, W. Liu, J. Xin and J. Zhang, *Macromolecules*, 2017, **50**, 8588–8597.
53 F. Chen, F. Gao, J. Zhong, L. Shen and Y. Lin, *Mater. Chem. Front.*, 2020, **4**, 2723–2730.
54 T. Vidil and A. Llevot, *Macromol. Chem. Phys.*, 2022, **223**, 2100494.
55 T. Liu, C. Hao, S. Zhang, X. Yang, L. Wang, J. Han, Y. Li, J. Xin and J. Zhang, *Macromolecules*, 2018, **51**, 5577–5585.
56 Y. Tao, L. Fang, M. Dai, C. Wang, J. Sun and Q. Fang, *Polym. Chem.*, 2020, **11**, 4500–4506.
57 A. Moreno, M. Morsali and M. H. Sipponen, *ACS Appl. Mater. Interfaces*, 2021, **13**, 57952–57961.
58 A. Adjaoud, L. Puchot and P. Verge, *ACS Sustainable Chem. Eng.*, 2022, **10**, 594–602.
59 M. Jasiński, L. Jasińska and M. Ogrodowczyk, *Cent. Eur. J. Urol.*, 2013, **66**, 144.
60 J. M. Sales and A. V. A. Resurreccion, *Crit. Rev. Food Sci. Nutr.*, 2014, **54**, 734–770.
61 W. Peng, R. Qin, X. Li and H. Zhou, *J. Ethnopharmacol.*, 2013, **148**, 729–745.
62 G. Chatel, R. Duwald, C. Piot and M. Draye, *Sci. Eaux Territ.*, 2019, **27**, 102.
63 H. Fretz, *Tetrahedron*, 1998, **54**, 4849–4858.
64 C. Chatalova-Sazepin, M. Binayeva, M. Epifanov, W. Zhang, P. Foth, C. Amador, M. Jagdeo, B. R. Boswell and G. M. Sammis, *Org. Lett.*, 2016, **18**, 4570–4573.
65 C. Aouf, C. Le Guernevé, S. Caillol and H. Fulcrand, *Tetrahedron*, 2013, **69**, 1345–1353.
66 Y. Tian, Q. Wang, L. Shen, Z. Cui, L. Kou, J. Cheng and J. Zhang, *Chem. Eng. J.*, 2020, **383**, 123124.
67 M. D. Garrison, M. A. Savolainen, A. P. Chafin, J. E. Baca, A. M. Bons and B. G. Harvey, *ACS Sustainable Chem. Eng.*, 2020, **8**, 14137–14149.
68 Y. Tian, M. Ke, X. Wang, G. Wu, J. Zhang and J. Cheng, *Eur. Polym. J.*, 2021, **147**, 110282.
69 H. Liu, H. Zhang, H. Wang, X. Huang, G. Huang and J. Wu, *Chem. Eng. J.*, 2019, **368**, 61–70.
70 M. Giebler, C. Sperling, S. Kaiser, I. Duretek and S. Schlögl, *Polymers*, 2020, **12**, 1148.
71 F. Gamardella, F. Guerrero, S. De la Flor, X. Ramis and A. Serra, *Eur. Polym. J.*, 2020, **122**, 109361.
72 Y. Nishimura, J. Chung, H. Muradyan and Z. Guan, *J. Am. Chem. Soc.*, 2017, **139**, 14881–14884.